ADDRESSING SOURCES OF UNCERTAINTY IN ESTIMATING LIQUEFACTION-INDUCED GROUND SETTLEMENT

F. R. Olaya[1], J. D. Bray[2] & N. A. Abrahamson[3]

[1] University of California, Berkeley, California, United States

[2] University of California, Berkeley, California, United States, jonbray@berkeley.edu

[3] University of California, Berkeley, California, United States

Abstract: *Widely used methods to estimate liquefaction-induced ground settlement have been largely developed using a deterministic framework. In this paper, the recently developed Bray and Olaya (2023) probabilistic procedure to estimate liquefaction-induced ground settlement is incorporated in a performance-based procedure to estimate ground settlement while accounting for key sources of epistemic uncertainty. Performance-based procedures are preferred to state-of-practice procedures that treat the assessment of seismic demand and engineering response parameters independently. In this performance-based approach, the ground motion intensity and ground settlement estimations are integrated to produce alternative hazard curves for liquefaction-induced ground settlement. The resulting mean hazard curve for ground settlement links different hazard levels with their corresponding values of ground settlement by evaluating a wide range of ground motion intensities and ground characterization parameters with their epistemic uncertainties. In contrast to the approaches frequently used in practice, the performance-based procedure produces an estimate of liquefaction-induced ground settlement compatible with the specified design hazard level. Key sources of epistemic uncertainty are included in the evaluation of liquefaction-induced settlement hazard curve through a logic tree approach. The use of the proposed procedure is illustrated at a site in California. Post-liquefaction ground settlement estimates at this site were obtained deterministically for a controlling earthquake scenario and at two hazard levels (i.e., return periods of 475-year and 2475-year) using the performance-based approach. The performance-based procedure yields estimates of liquefaction-induced ground settlement consistent with the target hazard levels, whereas conventional approaches overestimate the liquefaction-induced ground settlement at the 475-year return period due to the different slopes of the ground motion and liquefaction-induced ground settlement hazard curves at this return period.*

1. Introduction

The accumulation of liquefaction-induced volumetric strains resulting from sedimentation and reconsolidation processes leads to ground settlement, S_v (e.g., Ishihara and Yoshimine 1992, Bray and Olaya 2023). These processes occur as excess pore water pressures dissipate and the soil's effective stress increase. Hence, volumetric strains are present whenever some amount of excess pore water pressure is generated. Estimation of the likely amount of post-liquefaction ground settlement is of practical importance because differential ground settlement induced by liquefaction can result in the failure of structures, buried structures, and roadways.

The M_w = 9.1 2011 Tohoku earthquake produced extensive liquefaction in Urayasu in Japan. The reconnaissance effort by Tokimatsu et al. (2012) documented different mechanisms of liquefaction-induced ground settlement (e.g., Bray and Macedo 2017). Figure 1 shows the amplitude of liquefaction-induced settlement of the ground adjacent to a pile-supported building. The building in Figure 1 was supported by a deep foundation system with the pile group's neutral plane (i.e., the depth at which the pile and soil settlement are equal) below the liquefied soil. Soil layers above the neutral plane have already loaded the pile with downward soil movement. Inspection of the building indicated that no vertical movement occurred because of liquefaction while the adjacent ground settled about 30 cm relative to the pile-supported building. This amount of liquefaction-induced volumetric ground settlement was widespread in the free-field areas of Urayasu. It made access to the buildings difficult and damaged the connections of buried utilities that settled with the ground in which they were embedded.

Currently, dynamic nonlinear effective stress analyses using continuum-based methods do not capture sedimentation and reconsolidation processes effectively. Hence, the estimation of liquefaction-induced ground settlement relies largely on empirical methods. However, currently available empirical methods have been largely based on a limited number of case histories (e.g., Zhang et al. 2002). To overcome this limitation, Olaya and Bray (2023) develop a database of 205 well-documented field case histories of liquefaction-induced ground settlement characterized by the cone penetration test (CPT). This database classifies the sites as natural soil deposit or hydraulic fill sites to account for their different geological formation processes and their different seismic performance. The Olaya and Bray (2023) database of field case histories brings in information from a wide range of soil conditions, ground motion intensities, and varying degrees of liquefaction severity. The database provides a robust basis to evaluate the mechanisms and amplitude of post-liquefaction ground settlement as well as to assess the variability in its estimation.

In current practice, the procedures to assess liquefaction-induced ground settlement (S_v) are either deterministic or pseudo-probabilistic (Rathje and Saygili 2008) where the ground motion intensity measure (IM) and S_v are computed separately. In the deterministic approach, the IM is obtained from an earthquake scenario consisting of the M_w, source-to-site distance (R), and the number of standard deviations above the median ground motion (epsilon - ε). Subsequently, S_v is estimated from empirical models that are usually a function of the soil's relative density (D_r) and the factor of safety against liquefaction (FS_L) computed using the M_w and IM defined by the selected earthquake scenario. In a pseudo-probabilistic approach, a hazard curve for the IM (λIM) is developed through a probabilistic seismic hazard assessment (PSHA) that combines the contribution from all relevant earthquake scenarios (e.g., M_w, R, and ε). A design hazard level (or return period) is prescribed, and the corresponding IM value is selected to represent the seismic demand. S_v is then estimated using an empirical model with the D_r of the soil deposit and the FS_L computed using the selected IM and its hazard-consistent M_w. In the pseudo-probabilistic approach, it is implicitly assumed the selected design hazard level of the IM (λIM) is the same as the hazard level for S_v. However, as will be demonstrated in this paper, this assumption is not always valid.

In a performance-based earthquake engineering (PBEE) approach, the hazard evaluation for the IM is incorporated explicitly in the assessment of S_v by combining λIM with the probability of exceeding different S_v levels. Hence, the variability in the estimate of λIM is incorporated directly in the evaluation of S_v. In addition, the uncertainty of the inputs to the model for S_v can also be included in a performance-based evaluation. The objective of a performance-based approach is to construct the mean hazard curve for S_v [i.e., $\lambda(S_v)$]. Then, different fractiles of $\lambda(S_v)$ can be explored, if required, by including information on sources of epistemic uncertainty relevant to the calculation of S_v. The hazard curve for S_v enables alternative hazard levels (or return periods) for S_v to be evaluated simultaneously in contrast to the pseudo-probabilistic approach where they are calculated separately.

In this paper, the application of a performance-based procedure for the assessment of S_v is presented. The proposed procedure is described, and key aspects of its formulation are presented. The use of the proposed procedure is illustrated for a site in California. Post-liquefaction ground settlement estimates at this site were obtained deterministically for a controlling earthquake scenario, pseudo-probabilistically for two hazard levels (i.e., return periods of 475-year and 2475-year), and using the performance-based approach that considers a wide range of hazard levels. Key insights are shared, and recommendations for the use of the proposed PBEE liquefaction-induced ground settlement procedure are made.

Figure 1. Free-field ground settlement of liquefied soil relative to pile supported building that derives its support from soil layers below the liquefiable soil (adapted from Tokimatsu et al. 2012).

2. Probabilistic model for liquefaction-induced ground settlement

Ishihara and Yoshimine (1992) developed a procedure for estimating post-liquefaction ground settlement that employs a laboratory-based model to estimate volumetric strain (ε_v), the standard penetration test (SPT) or cone penetration test (CPT) to estimate soil density, and a SPT or CPT liquefaction triggering procedure to estimate the factor of safety of liquefaction triggering (FS_L). Post-liquefaction volumetric strains are calculated as a function of the estimated D_r and FS_L values of each layer in the soil profile. In the Ishihara and Yoshimine procedure, S_v is calculated from the accumulation of settlement of each soil layer that develops within a free-field soil deposit due to the post-liquefaction-induced volumetric strain in the layer multiplied by its thickness.

The probabilistic liquefaction-induced free-field ground settlement procedure of Bray and Olaya (2023) follows the framework of the Ishihara and Yoshimine (1992) procedure, but instead it uses the empirical model for ε_v of the Olaya and Bray (2022) laboratory-based model, relies on the CPT to estimate D_r, and is calibrated using the well-documented CPT database of 205 field case histories of liquefaction-induced ground settlement of Olaya and Bray (2023). The Bray and Olaya (2023) probabilistic model is summarized in Equations 1, 2, and 3.

$$S_v = C \cdot MF \cdot SB \cdot \sum_i [\varepsilon_{vi} \cdot \Delta z_i] \cdot e^{\delta_{S_v}} \quad (1)$$

$$SB = \exp\left(-0.675 \cdot \max\left(I_{c_{15}}, 1.8\right) + 1.215\right) \quad (2)$$

$$MF = \exp(0.214 \cdot M_w - 1.498) \quad (3)$$

where C (a calibration factor) = 1.50 for natural soil and C = 1.05 for hydraulic fill, ε_{vi} (as a decimal) is the volumetric strain of each soil layer i with thickness Δz_i, and δ_{S_v} is the residual term of the model which has zero mean and a standard deviation of 0.54 in natural log units for hydraulic fill and 0.61 in natural log units for natural soil for the D_r-based volumetric-strain model. The soil behavior factor (*SB*) captures the trend of ground settlement reducing as the average soil behavior type index (I_c) (Robertson 2009) over the upper 15 m of the soil profile (I_{c15}) increases. The magnitude factor (*MF*) captures the increase in ground settlement due to additional cycles of loading after liquefaction is triggered which is correlated the duration of strong shaking, which is captured with moment magnitude (M_w).

The term $\Sigma_i[\varepsilon_{v,i} \cdot \Delta z_i]$ in Equation 1 represents the cumulative contribution of volumetric strain with depth in the soil profile, which has been divided into layers. $\varepsilon_{v,i}$ is estimated from the median values of the Olaya and Bray (2022) model, hence the term $\Sigma_i[\varepsilon_{v,i} \cdot \Delta z_i]$ is representative of a median quantity. As a result of using the median value, the aleatory variability of $\Sigma_i[\varepsilon_{v,i} \cdot \Delta z_i]$ about the median is captured in the residual δ_{Sv}.

The model uses the unbiased FS_L at a probability of liquefaction triggering (P_L) of 50% calculated using the average of two simplified liquefaction triggering procedures: (1) the Robertson and Wride (1998) procedure as updated by Robertson (2009) and converted to a probabilistic method by Ku et al. (2012), and (2) the Boulanger and Idriss (2016) probabilistic procedure. To estimate the soil D_r, the average of the CPT-based correlations for D_r of Bray and Olaya (2023) and Robertson and Cabal (2015) are used. Alternative liquefaction triggering procedures or correlations for D_r can alter the estimate of S_v in a manner dependent on the procedure or correlation employed.

3. Performance-based evaluation of liquefaction-induced ground settlement

The annual rate at which a given amount of liquefaction-induced free-field ground settlement (z) is exceeded ($S_v > z$) for a given level of *IM* at a site can be evaluated within the PBEE framework developed at the Pacific Earthquake Engineering Research Center (PEER) (Deierlein et al. 2003). The information from the PSHA is convolved with an empirical model for S_v to produce the hazard curve for post-liquefaction ground settlement $\lambda(S_v)$ using Equation 4.

$$\lambda(S_v > z) = \int_{M_w}\int_{PGA} P(S_v > z|PGA, M_w, I_{c15},\ \Sigma_i[\varepsilon_{v,i} \cdot \Delta z_i])\, f(M_w|PGA) \left|\frac{d\lambda_{PGA}}{d(PGA)}\right| d(PGA)dM_w \tag{4}$$

where $P(S_v > z|PGA, M_w, I_{c15},\ \Sigma_i[\varepsilon_{v,i} \cdot \Delta z_i])$ is the probability that a ground settlement z is exceeded conditioned on *PGA*, M_w, I_{c15}, and $\Sigma_i[\varepsilon_{v,i} \cdot \Delta z_i]$, $f(M_w|PGA)$ is the probability density function for M_w given the *PGA*, and $|d\lambda_{PGA}/d(PGA)|$ is the derivative of the hazard curve for *PGA*. The $f(M_w|PGA)$ term captures the contribution of different M_w scenarios to the seismic hazard for *PGA* and can be obtained from the seismic hazard deaggregation for *PGA.* The computation of Equation 4 for different values of ground settlement produces the hazard curve for S_v. The PEER PBEE methodology has been successfully applied to evaluate a variety of geotechnical problems (e.g., Mayfield et al. 2010 and Kramer 2013).

4. Key sources of uncertainty in estimating liquefaction-induced ground settlement

The sources of uncertainty in the performance-based assessment of S_v are categorized as either aleatory variability or epistemic uncertainty following the convention used in seismic hazard evaluations. The aleatory variability is characterized by the standard deviation of the ground motion models considered in the PSHA and by the standard deviation of the empirical model employed to estimate S_v (i.e., Equation 1). The uncertainty related to the soil characterization parameters that are inputs to the S_v model (i.e., parameters derived from CPT soundings within a site) is treated as epistemic and evaluated using a logic-tree approach that produces alternative hazard curves. The main CPT measurements are the corrected cone tip resistance (q_t) and the sleeve friction (f_s), which are used as inputs to the correlations to estimate D_r and to the liquefaction triggering procedures to calculate FS_L. Subsequently, ε_v is estimated as a function of D_r and FS_L using the Olaya and Bray (2022) model described previously.

In the Bray and Olaya (2023) S_v model, the ε_v contribution from all layers, $\Sigma_i[\varepsilon_{v,i} \cdot \Delta z_i]$, and the average soil behavior for a site, I_{c15}, are components of the model (Equations 1 and 2). Hence, alternative values of q_t and f_s will produce alternative values of I_{c15} and $\Sigma_i[\varepsilon_{v,i} \cdot \Delta z_i]$ in the Bray and Olaya (2023) S_v model. Therefore, logic trees for I_{c15} and $\Sigma_i[\varepsilon_{v,i} \cdot \Delta z_i]$ can be used to capture the epistemic uncertainty in the soil characteristics of a site measured through the q_t and f_s parameters. Reference values of the epistemic uncertainty in I_{c15} and $\Sigma_i[\varepsilon_{v,i} \cdot \Delta z_i]$ in the form of the coefficient of variation (*COV*) values are obtained by analysing the case histories reported in the Olaya and Bray (2023) database as shown in Table 1. The ranges of COV are estimated from sites with at least 4 CPTs.

Table 1. COV for I_{c15} and $\Sigma[\varepsilon_{v,i} \cdot \Delta z_i]$ in terms of I_{c15}.

		Natural Soil	**Hydraulic Fill**
***COV* (I_{c15})**	$I_{c15} < 1.8$	0.01 - 0.04	-
	$1.8 \le I_{c15} < 2.2$	0.03 - 0.05	0.02
	$I_{c15} \ge 2.2$	0.03 - 0.05	0.04
***COV* ($\Sigma[\varepsilon_{v,i} \cdot \Delta z_i]$)**	$I_{c15} < 1.8$	0.10 - 0.40	-
	$1.8 \le I_{c15} < 2.2$	0.10 - 0.30	0.10 - 0.20
	$I_{c15} \ge 2.2$	0.20 - 0.40	0.20 - 0.30

The effect of the epistemic uncertainty in λ_{IM} and S_v is illustrated through a simplified PSHA for two seismic sources in a crustal seismic setting where three alternative characteristic magnitudes, two annual activity rates, and one rupture location for each fault are considered as shown in Table 2. Two ground motion models (GMMs) with different medians and standard deviations were utilized to estimate the *PGA* at the site. Given the alternative M_w, rates, and GMMs, a total of 72 alternative hazard curves for *PGA* were developed.

Table 2. Epistemic uncertainty in the PSHA.

Fault 1		**Fault 2**	
M_w	**Rate**	**M_w**	**Rate**
7.5 (0.2)	1/300 (0.5)	6.75 (0.2)	1/1000 (0.7)
7.25 (0.6)	1/150 (0.5)	6.5 (0.6)	1/3000 (0.3)
7 (0.2)		6.25 (0.2)	

Note: The values in parenthesis are the assigned weights to each alternative value.

The epistemic uncertainty in the soil characterization was estimated from Table 1 considering a natural soil deposit. For the parameter I_{c15}, a *COV* of 0.04 is used and for the term $\Sigma_i[\varepsilon_{v,i} \cdot \Delta z_i]$, a COV of 0.20 is used. Five-branch logic trees with branch values of -2, -1, 0, 1, and 2 epsilons and weights of 0.065, 0.24, 0.39, 0.24, and 0.065 for I_{c15} and $\Sigma_i[\varepsilon_{v,i} \cdot \Delta z_i]$ are used to better capture the epistemic fractiles of the S_v hazard for a nonlinear system (relative to the conventional three-branch logic tree). The mean I_{c15} for this example is 1.82 whereas the $\Sigma_i[\varepsilon_{v,i} \cdot \Delta z_i]$ term varies depending on the M_w and *PGA* scenario being analyzed. The convolution of the 72 alternative hazard curves for *PGA* with the alternative realizations of the Bray and Olaya (2023) model for S_v model using the five-branch logic tree produces 1800 hazard curves for S_v, All hazard curves are shown in Figure 2 with the mean hazard curve, median hazard curve, and the 16th and 84th percentile fractiles.

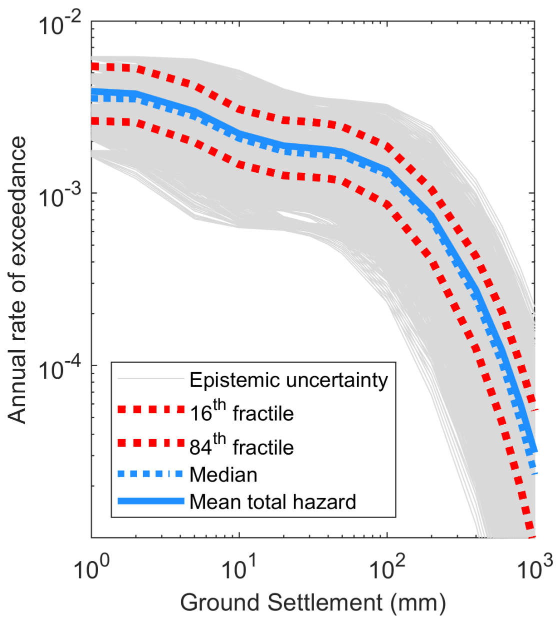

Figure 2. Alternative liquefaction-induced free-field ground settlement hazard curves.

5. Performance-based evaluation of liquefaction-induced ground settlement

The performance-based evaluation of ground settlement can be summarized in four steps:

1. Perform a seismic hazard evaluation at the site of interest obtaining the mean hazard curve for *PGA* and the deaggregation for different M_w bins at *PGA* values up to 10 *g*.
2. To address the uncertainty in the estimation of S_v, evaluate the epistemic uncertainty of the soil parameters at the site in terms of I_{c15}. The epistemic uncertainty may be estimated from 3 or more representative CPTs performed at the site. The *COV* ranges provided in Table 1 can be used in the evaluation of the epistemic uncertainty to consider in cases when fewer CPTs are available or as a guide in performing site-specific estimates.
3. Equation 4 is used to compute $\lambda(S_v)$. It is recommended to evaluate settlement values of at least 1000 mm to ensure that low hazard levels (e.g., 10^{-5}) are captured. The epistemic uncertainty in the S_v estimation can be evaluated by including alternative values for I_{c15} and $\Sigma_i[\varepsilon_{v,i} \cdot \Delta z_i]$.
4. Select the return periods of interest. In engineering practice, return periods of 475 and 2475 years are often used to assess the seismic performance of the ground affecting new structures. Estimate the mean and 16th and 84th percentile fractiles of S_v at the selected return periods.

6. Example of the use of the performance-based liquefaction-induced ground settlement procedure

6.1. Site

The proposed performance-based procedure to evaluate liquefaction-induced free-field ground settlement is performed a site in eastern California to illustrate its use and to share insights gained from employing this new approach. Four CPTs are available to explore the soil profile characteristics at the site as illustrated in Figure 3. The soil at the site is composed of crust material (thickness of 2 m to 3 m) followed by uniform thick layers of clean sands and silty sands with the I_c fluctuating around I_c = 1.8 with a representative I_{c15} of 1.86. At a depth of about 12 m, there is a thin layer of clayey material, and a layer of siltier soil is located at depth of 18-19 m. The groundwater table is located at a depth of 2 m. The normalized cone tip resistance increases with depth, and the soil layers between depths of 2 m to 13 m contribute the most to the potential for liquefaction-induced settlement as can be seen from the distribution of FS_L in Figure 3, which was calculated using the 475-year return period *PGA* estimated at the site.

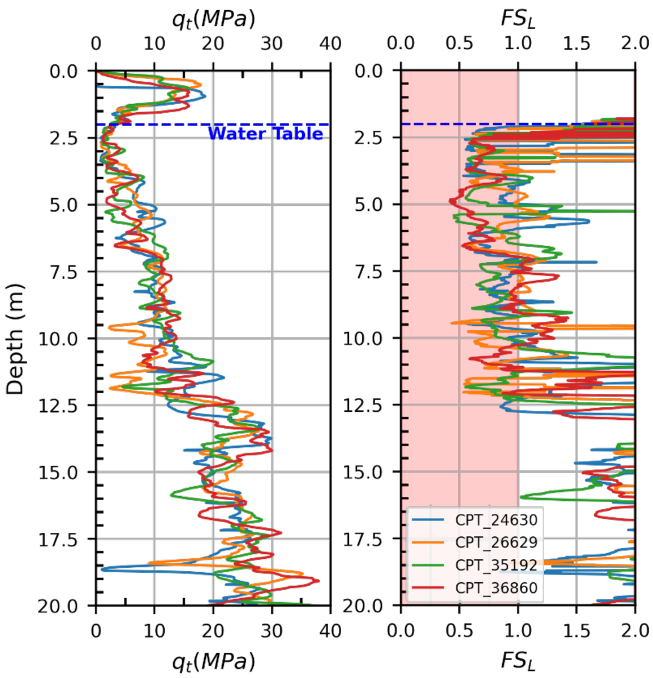

Figure 3. CPT cone tip resistance (q_t) data at test site with the calculation of the FS_L using the PGA at the 475-year return period.

6.2. PSHA

The PSHA was performed with the open-source software *Haz45.V3* (Abrahamson 2020). Initially, the performance-based evaluation for S_v was performed using Equation 1 and CPT_24630 that is representative of the average soil characteristics at the site, and which leads to an estimate of the mean $\lambda(S_v)$. Figure 4 shows the comparison between the mean hazard curve for PGA (Figure 4a) and the mean hazard curve for S_v (Figure 4b). The 475-year and 2475-year return periods are superimposed for reference. The curvatures of the two hazard curves differ, particularly at short return periods where the $\lambda(S_v)$ curve is relatively flat due to the negligible liquefaction triggered at the site for ground motions with PGA less than about 0.12 g. A steep $\lambda(S_v)$ curve is observed at long return periods because at high PGAs the site liquefies regardless of the PGA with S_v approaching a limiting value. As a result, the aleatory variability of $\lambda(S_v)$ at long return periods results mainly from the standard deviation of the ground motion model (σ_{GM}).

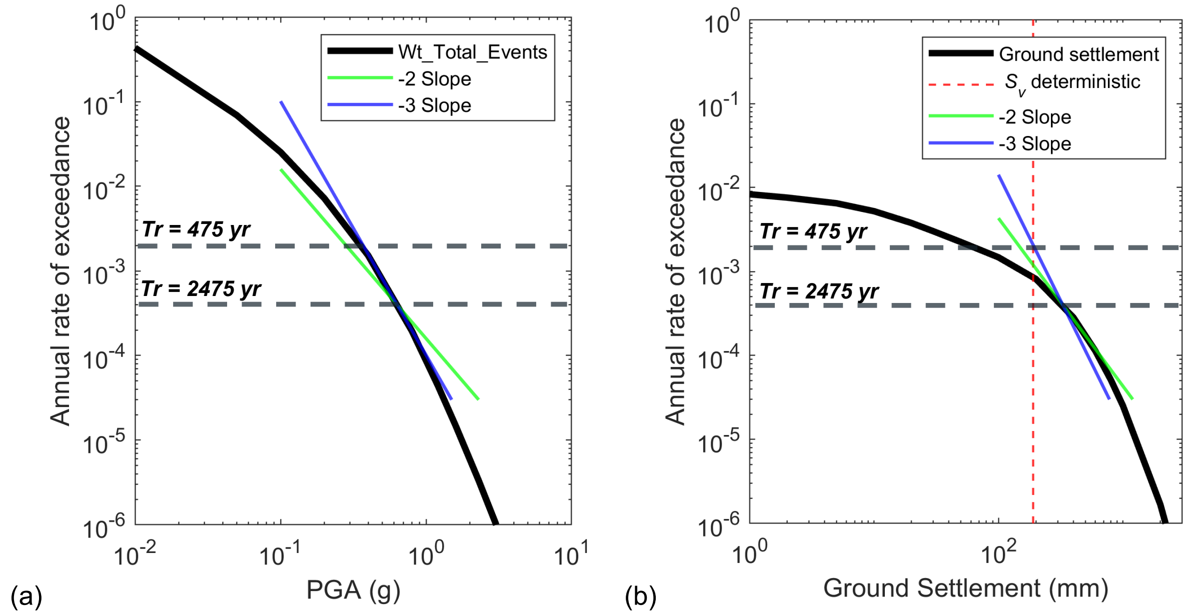

Figure 4. Mean total hazard curve for PGA, and (b) mean hazard curve for S_v at the test site.

6.3. Comparison of liquefaction-induced ground settlement estimates

A comparison of the liquefaction-induced ground settlement values estimated using a deterministic procedure, the pseudo-probabilistic procedure wherein a PSHA is used to select the PGA value used in the analysis, and the proposed performance-based procedure is insightful. In this application, comparisons are made at the commonly selected 475-year and 2475-year return periods.

The earthquake scenario for the deterministic analysis is M_w = 6.2 and R = 7.5 km, based on the source that generates the highest 84th percentile estimate of *PGA* at the site. The 84th percentile (or ε = 1.0) ground motion intensity measure is often used to consider the variability in the *IM* estimation for critical infrastructure. The deterministic *PGA* at the site was evaluated using the Abrahamson et al. (2014) GMM with ε = 1.0. The deterministic estimate of S_v = 190 mm is shown as a vertical line in Figure 4b.

In the pseudo-probabilistic procedure, the input *PGA* and M_w values at the return periods of interest are first obtained from a PSHA. The resulting *PGAs* at this site are 0.30 *g* and 0.60 *g* for the 475-year and 2475-year return periods, respectively, with the controlling M_w of 6.2 and 6.4, respectively. In a performance-based procedure, ground settlement is obtained directly from the hazard curve for S_v (Figure 4b). There is no separation of estimating the *PGA* at a hazard level, and then estimating the S_v value for that particular *PGA* value.

A summary of the estimated liquefaction-induced ground settlement values using the three procedures are summarized in Table 3. The pseudo-probabilistic procedure estimates a higher S_v value of 90 mm relative to the performance-based procedure of S_v = 65 mm at the 475-year return period. At this return period at the site, the pseudo-probabilistic procedure produces a mean S_v value that is 40% greater than the mean estimate of S_v using the performance-based procedure because the pseudo-probabilistic procedure does not capture correctly the *PGA* and M_w scenarios that contribute to the hazard for settlement. The pseudo-probabilistic and performance-based procedures provide similar estimates of S_v at the 2,475-year return period with the slopes of the hazard curves for PGA and S_v being also similar. The performance-based assessment of S_v can also be used to provide context for the hazard associated with the deterministic estimate of S_v. The 84th percentile *PGA* deterministic estimate of S_v is associated with a return period of about 1200 years (Figure 4b). Hence, the deterministically computed liquefaction-induced ground settlement using the 84th percentile (ε = 1.0) ground motion intensity measure from a controlling earthquake scenario does not produce a 'worst case' estimate of S_v as it is sometimes assumed in engineering practice.

Table 3. Ground settlement estimation using the pseudo-probabilistic and performance-based procedures. As a reference, the deterministic estimate using the 84th percentile PGA is S_v = 190 mm.

Return Period (year)	S_v (mm)	
	Pseudo-Probabilistic Procedure	**Performance-Based Procedure**
475	90	65
2500	310	300

6.4. Epistemic uncertainty examination

This example also illustrates the effects of considering epistemic uncertainty in the soil parameters by using alternative values for the site characterization terms of I_{c15} and $\Sigma_i[\varepsilon_{v,i} \cdot \Delta z_i]$. The four CPTs at the site provide estimates of site characterization uncertainty as *COV*(I_{c15}) = 0.02 and *COV*($\Sigma_i[\varepsilon_{v,i} \cdot \Delta z_i]$) = 0.15. The sensitivity of the results to these *COV* values is explored by also using the upper limits of COV(I_{c15}) = 0.05 and *COV*($\Sigma_i[\varepsilon_{v,i} \cdot \Delta z_i]$) = 0.30 in Table 1.

The resulting range in $\lambda(S_v)$ is shown in Figure 5. Epistemic uncertainty in I_{c15} does not significantly affect the liquefaction-induced ground settlement hazard curve as shown in Figure 5a. The hazard curves for *COV*(I_{c15}) = 0.02 and 0.05 differ only slightly. This occurs because I_{c15} has minimum values of 1.79 and 1.67 for COVs of 0.02 and 0.05 respectively, for which *SB* in Equation 2 has a value of 1.0 (I_{c15} < 1.80); thus, similar values of $\lambda(S_v)$ are calculated. Conversely, the epistemic uncertainty in $\Sigma_i[\varepsilon_{v,i} \cdot \Delta z_i]$ has a significant effect on the S_v hazard curve at long return periods as depicted in Figure 5b. Increasing the *COV*($\Sigma_i[\varepsilon_{v,i} \cdot \Delta z_i]$) from 0.15 to 0.30 approximately doubles the range of the estimated liquefaction-induced ground settlement.

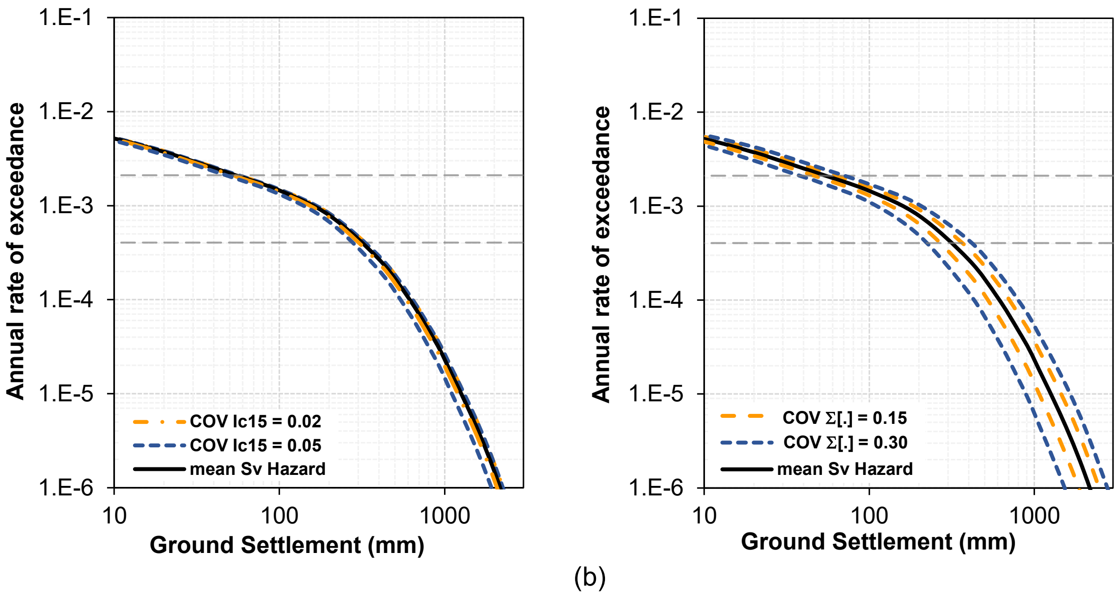

Figure 5. Effect of epistemic uncertainty of soil characterization on the $\lambda(S_v)$: (a) uncertainty in I_{c15}, and (b) uncertainty in $\Sigma_i[\varepsilon_{v,i} \cdot \Delta z_i]$.

7. Conclusions

A performance-based procedure to estimate post-liquefaction-induced ground settlement is developed in which the hazard evaluation for the ground motion intensity measure is incorporated in the estimate of the ground settlement by combining the hazard curve for the *IM* with the probability of exceeding different S_v levels. By doing so, the sources of variability contributing to the *IM* are incorporated in the estimate of S_v. The primary inputs to the proposed performance-based procedure are the mean seismic hazard curve for *PGA*, the deaggregation information by magnitude at different *PGA* values, the CPT data at the site, and the empirical model of Bray and Olaya (2023) for estimating free-field liquefaction-induced ground settlement.

The variability of the geotechnical characterization parameters used in the empirical model for S_v are captured using logic-trees. The effects of the epistemic uncertainty of the geotechnical characterization of a site can be assessed through examining how their uncertainty (i.e., *COV* values) modify the liquefaction-induced ground settlement hazard curves. For the site examined in this paper, the epistemic uncertainty in the calculation of $\Sigma_i[\varepsilon_{v,i} \cdot \Delta z_i]$ has a significant effect on the S_v hazard curve at long return periods, whereas the epistemic uncertainty of the parameter I_{c15} does not affect the results significantly.

Pseudo-probabilistic procedures decouple the assessment of seismic demand (i.e., *PGA*) and the engineering response parameter (i.e., S_v). A pseudo-probabilistic procedure assumes wrongly the selected design hazard level of the IM is consistent with the hazard level for the engineering demand parameter of S_v. Thus, it can provide estimates of S_v that are inconsistent with the actual hazard-consistent estimate of S_v as shown in the example where it overestimated the liquefaction-induced ground settlement by 40% at the 475-year return period.

The deterministic procedure provides an arbitrary estimate of S_v because it considers only one earthquake scenario with one value of the *IM* at a predetermined percentile of the *IM* estimate. The selection of the percentile of the *IM* estimate is arbitrary and its choice can lead to a wide range of hazard levels of S_v. The deterministic procedure should be used with caution in engineering practice.

Conversely, the proposed performance-based procedure is recommended for use in engineering practice because it delivers estimates of liquefaction-induced ground settlement consistent with the target hazard levels and enables the evaluation of different sources of epistemic uncertainty and their effects on liquefaction-induced ground settlement.

8. Acknowledgements

Support for this research was provided primarily by the U.S. National Science Foundation (NSF) through grant CMMI-1956248. The findings, opinions, and conclusions presented in this paper are those of the authors and do not necessarily reflect the views of the NSF. The College of Engineering at the University of California, Berkeley (UCB) provided additional support through the Faculty Chair in Earthquake Engineering Excellence.

9. References

Abrahamson, N. A. (2020). Haz45 computer program. https://github.com/abrahamson/HAZ. (Last accessed June 2020).

Abrahamson N.A., Silva W.J., Kamai R. (2014). Summary of the ASK14 ground motion relation for active crustal regions. *Earthq Spectra* 30(3):1025-1055.

Boulanger R.W., Idriss I.M. (2016). CPT-based liquefaction triggering procedures. *J Geotech Geoenviron Eng.*, ASCE, 142(2), 04015065.

Bray, J., Macedo, J. (2017). Simplified procedure to estimate liquefaction induced building settlements. 6th Ishihara Lecture. Soil dynamics and earthquake engineering; 102:215-231.

Bray J.D., Olaya F.R. (2023). 2022 H. Bolton Seed Medal Lecture - Evaluating the Effects of Liquefaction. *J Geotech Geoenviron Eng.*, ASCE, 149(8), doi: 10.1061/JGGEFK.GTENG-11242.

Deierlein, G., Krawinkler, H., and Cornell, C., (2003). A framework for performance-based earthquake engineering, *Pacific Conf. EQ Eng*, 13–15 Feb, Christchurch, New Zealand.

Ishihara K, and Yoshimine M. (1992). Evaluation of settlements in sand deposits following liquefaction during earthquakes. *Soils Found.*, 32(1),173–188.

Kramer, S. L. (2013). Performance-based methodologies for geotechnical earthquake engineering, *Bull Earthquake Eng*. 1049–1070.

Ku C.S., Juang, C. H., Chang, C. W., and Ching J. (2012). Probabilistic version of the Robertson and Wride method for liquefaction evaluation: development and application. *Canadian Geotechnical J.*, 49(1), 27-44.

Mayfield, R. T., S. L. Kramer, and Y. M. Huang. (2010). Simplified approximation procedure for performance-based evaluation of liquefaction potential. *J. Geotech. Geoenviron. Eng*. 136 (1): 140–150.

Olaya F.R., and Bray J.D. (2022). Strain potential of liquefied soil. *J Geotech Geoenviron Eng*., ASCE, 148 (11): 04022099.

Olaya F.R., and Bray J.D. (2023). Post-liquefaction free-field ground settlement case histories. *Int*. *J of Geoeng. Case histories*., ISSMGE, 7(3), 18-33.

Rathje, E. M., and Saygili, G., (2008). Probabilistic seismic hazard analysis for the sliding displacement of slopes: scalar and vector approaches, *J. Geotech. Geoenviron. Eng*, ASCE 134(6), 804–814.

Robertson P.K. (2009). Performance-based earthquake design using the CPT. *Inter Conf Performance-Based Design in Earthquake Geotechnical Engineering* (Is-Tokyo 2009).

Robertson P.K., and Cabal K.L. (2015). Guide to CPT for geotechnical engineering, 6th ed., *Gregg Drilling Testing, Inc*. Signal Hill, CA.

Robertson P.K., and Wride C.E. (1998). Evaluating cyclic liquefaction potential using the Cone Penetration Test, *Can. Geotech. J*., 35(3):442–459.

Tokimatsu K, et al. (2012) Quick report on geotechnical problems in the 2011 Tohoku Pacific Ocean earthquake. Research reports on earthquake engineering, CUEE. #118. Tokyo Institute of Technology; 2011. p. 21–47. [in Japanese].